F³OCUS - Federated Finetuning of Vision-Language Foundation Models with Optimal Client Layer Updating Strategy via Multi-objective Meta-Heuristics

Pramit Saha
University of Oxford
pramit.saha@eng.ox.ac.uk

Felix Wagner
University of Oxford
felix.wagner@eng.ox.ac.uk

Divyanshu Mishra
University of Oxford
divyanshu.mishra@eng.ox.ac.uk

Can Peng
University of Oxford
can.peng@eng.ox.ac.uk

Anshul Thakur
University of Oxford
anshul.thakur@eng.ox.ac.uk

David Clifton
University of Oxford; Oxford-Suzhou Centre for Advanced Research
david.clifton@eng.ox.ac.uk

Konstantinos Kamnitsas
University of Oxford; Imperial College London; University of Birmingham
konstantinos.kamnitsas@eng.ox.ac.uk

J. Alison Noble
University of Oxford
alison.noble@eng.ox.ac.uk

Abstract

Effective training of large Vision-Language Models (VLMs) on resource-constrained client devices in Federated Learning (FL) requires the usage of parameter-efficient fine-tuning (PEFT) strategies. To this end, we demonstrate the impact of two factors viz., client-specific layer importance score that selects the most important VLM layers for finetuning and inter-client layer diversity score that encourages diverse layer selection across clients for optimal VLM layer selection. We first theoretically motivate and leverage the principal eigenvalue magnitude of layerwise Neural Tangent Kernels and show its effectiveness as client-specific layer importance score. Next, we propose a novel layer updating strategy dubbed F³OCUS that jointly optimizes the layer importance and diversity factors by employing a data-free, multi-objective, meta-heuristic optimization on the server. We explore 5 different meta-heuristic algorithms and compare their effectiveness for selecting model layers and adapter layers towards PEFT-FL. Furthermore, we release a new MedVQA-FL dataset involving overall 707,962 VQA triplets and 9 modality-specific clients and utilize it to train and evaluate our method. Overall, we conduct more than 10,000 client-level experiments on 6 Vision-Language FL task settings involving 58 medical image datasets and 4 different VLM architectures of varying sizes to demonstrate the effectiveness of the proposed method.

1. Introduction

Large Vision-Language Models (VLMs) have made significant advancements in multi-modal learning, excelling in tasks like Visual Question Answering (VQA) [9, 35, 45, 46, 51]. Their effectiveness stems from their extensive parameters often reaching millions or billions, allowing them to learn complex representations of image and text data. Fine-tuning these models with task-specific data is crucial for adapting them to specialized applications. However, gathering diverse training data centrally is challenging, especially in fields like healthcare, where strict privacy regulations prevent data aggregation across different centers. To address the privacy concerns, Federated Learning (FL) [2, 34, 47, 55] allows models to be trained directly on local devices, such as in healthcare clinics, without sharing sensitive data. Yet, fine-tuning large models locally is difficult due to limited computational power and smaller datasets, which hinders VLM adaptation.

(a) Existing layer selection methods
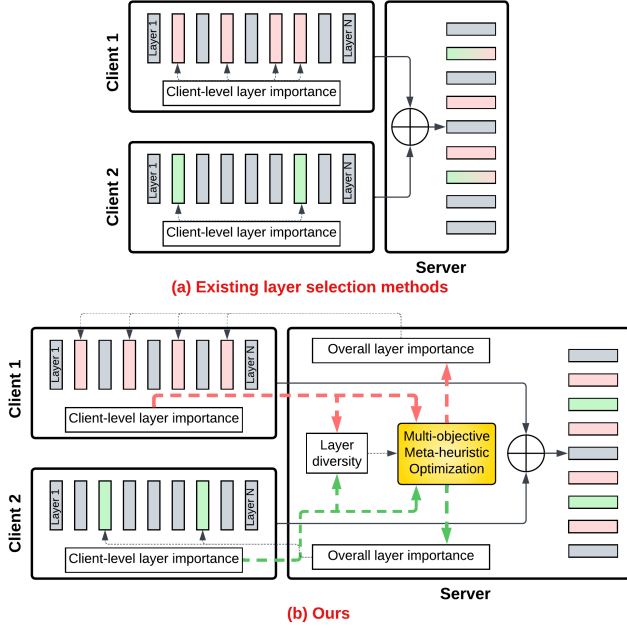
(b) Ours

Figure 1. Distinction of our approach from prior works. (a) illustrates vanilla layer-selection process, which only selects parameter subsets based on the local client data without considering the requirements of the other clients. (b) depicts our approach, F^3OCUS, which refines the client-specific layer selection by jointly maximizing overall client-specific importance score and layer selection diversity score across clients.

Balancing privacy with these resource limitations requires innovative solutions like Parameter-Efficient Fine-Tuning (PEFT) that fine-tunes either selected model parameters or added parameters while keeping the original model fixed [8, 24, 30, 32, 43, 48, 49, 60, 70]. Combined with FL, these offer a privacy-preserving and resource-efficient strategy for training large models collaboratively across multiple clients, particularly in computationally constrained settings.

Previous research [16, 65, 77, 79, 82, 87] has mostly focused on naive combination of centralized finetuning methods with FedAvg [55]. However, these works are primarily confined to single-modalities, addressing either visual or textual inputs independently. Besides, they do not consider the diverse characteristics and capacities of individual clients and typically assume homogeneous computational resources across all clients which is not applicable in most real-world collaborative settings. Hence, some clients either under-utilize the available resources or are unable to participate due to lack of compute. Our flexible layer selection PEFT-FL framework effectively addresses these issues.

The naive combinations of centralized selective PEFT methods [40, 42, 54, 61, 66, 72] and FL only consider local client data and task for selecting parameter subsets without considering other client requirements. This is especially
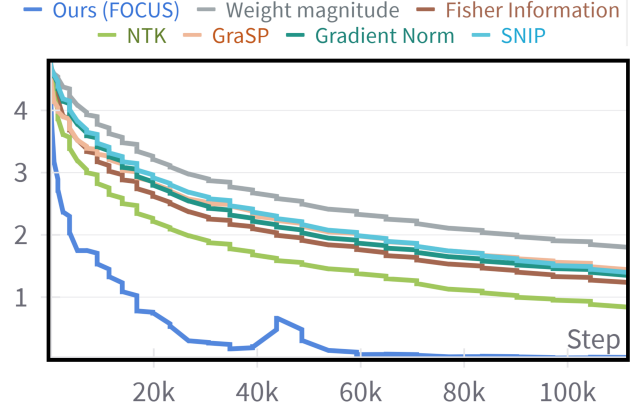

Figure 2. Loss convergence of layer selection methods. The gap between the client-specific NTK and FOCUS demonstrates the importance of our multi-objective meta-heuristic optimization.

problematic for FL clients facing challenges like heterogeneous modalities and computes, domain shifts, and statistical heterogeneity. In such cases, a poorly chosen client-specific configuration can not only slow down the overall convergence (see Fig. 2), but may also perform worse than training each client independently. Achieving the best performance requires a tailored approach that jointly considers client-specific as well as global optimization requirements.

To this end, we present a novel framework called F^3OCUS (**F**ederated **F**inetuning of **F**oundation Models with **O**ptimal **C**lient-specific Layer **U**pdating **S**trategy) to improve layer selection by considering both local and global FL characteristics while respecting the client-specific resource constraints. We propose a two-step "define and refine" procedure **at the beginning of every round**: (a) **client-level strategy**, that defines layer importance scores based on the principal eigenvalue of layerwise Neural Tangent Kernel (LNTK) and (b) **server-level strategy**, that refines client-specific layer selection by maximizing the overall client-specific importance scores while simultaneously minimizing the variance of the histogram of layer selections across clients, thereby promoting a more uniform distribution of layer participation. Our method (see Figs. 1 & 4) provides the clients with a flexible and dynamic solution for selecting layers where each client can specify their computational budgets, while ensuring faster convergence (see Fig. 2). In order to showcase the effectiveness of F^3OCUS, we conduct over **10,000** client-level experiments under **6** Vision-language FL task settings using **4** VLMs and 58 medical image datasets that involve **4** types of heterogeneities based on data, modality, device, and task. Our primary contributions can be summed up as follows:

- **Dataset contribution:** We release Ultra-MedVQA, **the largest medical VQA dataset to date,** consisting of **707,962** VQA triplets including **9** different modalities and

12 distinct anatomies, covering diverse open-ended and closed questions related to modality, tissue type, image view, anatomy, and disease (see Tab. 1 for comparison).

- **Technical contributions:** We theoretically motivate and propose F^3OCUS, a new selective layer fine-tuning strategy. We introduce LNTK-based client-level layer selection and server-level multi-objective meta-heuristic optimization that jointly optimizes client-specific layer importance score and inter-client layer diversity score. We theoretically motivate and analyze the effectiveness of our layer selection strategy and prove its convergence.

- **Empirical contributions:** Unlike previous works, we consider more constrained and realistic client settings involving data, modality, task, and device heterogeneity. We conduct comprehensive evaluations of F^3OCUS with 4 VLMs of varying sizes in diverse FL settings for tuning selective model layers as well as adapters. We empirically show that fine-tuning the last few adapters/layers of VLMs is only as good as tuning randomly selected adapters/layers. Consequently, we present detailed insights into F^3OCUS's performance improvements through: (a) analysis of client and server-based layer rank and importance score computation during training and (b) evaluation of different meta-heuristic optimization algorithms on the server *viz.*, Genetic Algorithm, Artificial Bee Colony, Ant Colony Optimization, Simulated Annealing, and Swarm Particle Optimization.

2. Background and Related works

Federated Learning (FL) FL enables various clients to collaboratively train models in a decentralized manner without sharing local data. The classical FL framework, FedAvg [55], offers a practical method for model aggregation. Several modifications have emerged to address the adverse impact of data heterogeneity in FL [2, 34, 47].

Centralized selective fine-tuning: Various methods have been explored for selecting subsets of parameters for fine-tuning foundation models in centralized training. These include optimizing non-structured mask matrices [36, 38, 39, 63, 76, 80, 83, 84], employing layer-wise selection [33, 36, 39, 42] and pruning methods [40, 44, 58, 72, 86].

Federated selective fine-tuning: Recent research has adapted these selective PEFT methods for FL [16, 28, 56, 84]. Specifically, studies by [22, 41] explore layer-wise network decomposition to facilitate selective model fine-tuning on client devices. Partial model personalization algorithms [13, 57] aim to train tailored subnetworks on clients to improve local models. However, these studies do not provide adaptive or dynamic layer selection strategies that consider the diverse characteristics of clients. Unlike prior works, we account for client-specific differences in resources and data distributions while also considering the global optimization requirements to perform selective layer fine-tuning.

3. Problem Formulation

Consider an FL system with a central server and N clients, represented by $\mathcal{N} = \{1, \ldots, N\}$. Each client has its own private dataset $\mathcal{D}_i$, containing $d_i = |\mathcal{D}_i|$ data points. The server contains a pre-trained foundation model parameterized by $\theta \in \mathbb{R}^P$, comprising L layers, indexed by $\mathcal{L} = \{1, 2, \ldots, L\}$. The server's objective is to fine-tune this model based on the clients' data $\{\mathcal{D}_i\}_{i \in \mathcal{N}}$ without directly accessing these datasets. The learning goal is formalized as:

$$\min_{\theta \in \mathbb{R}^P} F(\theta) = \sum_{i=1}^{N} \alpha_i F_i(\theta), \qquad (1)$$

where $\alpha_i = \frac{d_i}{\sum_{j=1}^{N} d_j}$ denotes relative sample size, and $F_i(\theta) = \frac{1}{d_i} \sum_{B_i \in \mathcal{D}_i} F_i(\theta; B_i)$ represents local training objective for client i, with $F_i(\theta; B_i)$ being the (potentially non-convex) loss function of model θ on data batch B_i. The FL training process proceeds over T rounds. In each round $t \in [T]$, the server selects a subset of clients $\mathcal{S}_t$ and distributes the updated global model θ_t to them for training.

Due to resource constraints, instead of the entire model, clients update only a subset of layers during local training. Each client-specific masking vector can be denoted as $m_{i,t} \in \{0,1\}^L$, where $m_{i,t}^l = 1$ if layer l is selected for training in round t, and $m_{i,t}^l = 0$ otherwise. Thus, the set of selected layers for client i at round t is denoted as $\mathcal{L}_{i,t} = \{l \in \mathcal{L} \mid m_{i,t}^l = 1\}$, and the union of all selected layers across clients in round t is $\mathcal{L}_t = \bigcup_{i \in \mathcal{S}_t} \mathcal{L}_{i,t}$.

Clients initialize their local models using global model from the server, $\theta_{i,t}$, and perform τ steps of local training using mini-batch SGD. For each local step $k \in [\tau]$, client i samples a batch of data $B_{i,t}$ and calculates gradients for the selected layers as:

$$\sum_{l \in \mathcal{L}_i^t} G_{i,l}(\theta_{i,t}^k; B_{i,t}^k) = \sum_{l \in \mathcal{L}_i^t} \nabla_l F_i(\theta_{i,t}; B_{i,t}), \qquad (2)$$

where $\nabla_l F(\theta)$ denotes the gradient of $F(\theta)$ with respect to the parameters of layer l. After computing the gradients, the local model is updated with learning rate η as:

$$\theta_{i,t}^k = \theta_{i,t}^{k-1} - \eta \sum_{l \in \mathcal{L}_i^t} G_i^l(\theta_{i,t}^{k-1}; B_{i,t}^{k-1}), \quad \forall k \in \{1, 2, \ldots, \tau\}, \qquad (3)$$

The accumulated weight update in one local round is:

$$\delta_{i,t} = \frac{1}{\eta}(\theta_{i,t}^0 - \theta_{i,t}^\tau) = \sum_{k=0}^{\tau-1} \sum_{l \in \mathcal{L}_i^t} G_i^l(\theta_{i,t}^k; B_{i,t}^k) \qquad (4)$$

Accumulated update after federated aggregation on server:

$$\delta_t = \sum_{i \in S_t} \sum_{k=0}^{\tau-1} \sum_{l \in \mathcal{L}_i^t} \alpha_i G_i^l(\theta_{i,t}^k; B_{i,t}^k) \qquad (5)$$

Table 1. # modalities (M) and VQA triplets in different datasets

	VQA-RAD	SLAKE	Path-VQA	VQA-Med	OmniMedVQA	Ours
# M	3	3	2	5	12	9
# VQA	3515	14028	32799	5500	127995	707962

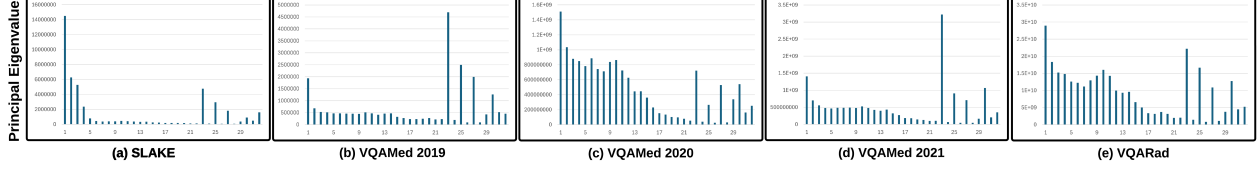
Figure 3. Visualization of principal eigenvalue magnitudes of LNTK (see §4.1) for computing layer importance score of LLaVA-1.5-7b

4. Client-level layer importance

4.1. Layerwise Neural Tangent Kernel (LNTK)

In this section, we first motivate the usage of LNTK towards prioritizing selected layers for client-specific fine-tuning. To capture the model training dynamics, consider the evolution of θ_t and training loss $\mathfrak{L}$ over input instances $\mathcal{X} \subset \mathcal{D}_i$:

$$\dot{\theta}_t = -\eta \nabla_\theta F(\mathcal{X}; \theta_t) \nabla_F(\mathcal{X}; \theta_t) \mathfrak{L}$$
$$\dot{\mathfrak{L}} = \nabla_F(\mathcal{X}; \theta_t) \mathfrak{L}^T \nabla_F(\mathcal{X}; \theta_t) \qquad (6)$$
$$\dot{\theta}_t = -\eta \nabla_F(\mathcal{X}; \theta_t) \mathfrak{L}^T \Theta(\mathcal{X}, \mathcal{X}) \nabla_F(\mathcal{X}; \theta_t) \mathfrak{L}$$

where the NTK matrix $\Theta_t(\mathcal{X}, \mathcal{X})$ at time t is defined as:

$$\Theta_t(\mathcal{X}, \mathcal{X}) \triangleq \nabla_\theta F(\mathcal{X}; \theta_t) \nabla_\theta F(\mathcal{X}; \theta_t)^T \in \mathbb{R}^{n \times n}. \qquad (7)$$

The integral NTK of a model [31] can be computed as the sum of layerwise NTK (LNTK), where we define LNTK as:

$$\Theta^l(\mathcal{X}, \mathcal{X}) = \nabla_{\theta^l} F(\mathcal{X}; \theta^l) \nabla_{\theta^l} F(\mathcal{X}; \theta^l)^T, \qquad (8)$$

where $\nabla_{\theta^l} F(\mathcal{X}; \theta^l)$ denotes the Jacobian of F at input points $\mathcal{X}$ with respect to the l-th layer parameters θ^l. The integral NTK can be expressed as: $\Theta(\mathcal{X}, \mathcal{X})$

$$\overset{(i)}{=} \sum_{l=1}^L \nabla_{\theta^l}(\mathcal{X}) \nabla_{\theta^l}(\mathcal{X})^T \overset{(ii)}{=} \sum_{l=1}^L \sum_{\theta_p \in \theta^l} \nabla_{\theta^l}(\mathcal{X}) \nabla_{\theta^l}(\mathcal{X})^T \overset{(iii)}{=} \sum_{l=1}^L \Theta^l(\mathcal{X}, \mathcal{X}) \qquad (9)$$

where (i) decomposes the matrix multiplication into the sum of vector multiplications; (ii) gathers addends by each module; and (iii) follows the definition of the LNTK. Since $\Theta^l(\mathcal{X}, \mathcal{X})$ is a positive semi-definite real symmetric matrix, we perform an eigen-decomposition of LNTK as:

$$\Theta^l(\mathcal{X}, \mathcal{X}) = U^l \Lambda^l (U^l)^T = \sum_{j=1}^{nk} \lambda_j^l u_j^l (u_j^l)^T \qquad (10)$$

where $\Lambda^l = \mathrm{diag}(\lambda_1^l, \lambda_2^l, \ldots, \lambda_{nk}^l)$ contains eigenvalues λ_j^l of $\Theta^l(\mathcal{X}, \mathcal{X})$, and each $\lambda_j^l \geq 0$. The mean output of the l-th layer in the eigenbasis of the LNTK can be described by:

$$(U^l E[\mathbf{f}^l(\mathcal{X})])_j = \left(I - e^{-\eta \lambda_j^l t} \right) (U^l y^l)_j \qquad (11)$$

where $\mathbf{f}^l(\mathcal{X})$ and y^l are actual and target l-th layer outputs. This formulation demonstrates that the convergence behavior of a layer is largely influenced by the eigenvalues λ_j^l of LNTK. Let $\lambda_1^l \geq \lambda_2^l \geq \cdots \geq \lambda_n^l$ denote the eigenvalues of $\Theta^l(\mathcal{X}, \mathcal{X})$, where λ_1^l is the principal eigenvalue. In particular, λ_1^l plays a dominant role in the convergence dynamics [10]. When using the largest possible layer-specific learning rate, $\eta^l \sim \frac{2}{\lambda_1^l}$, the training process aligns most strongly with the direction associated with the principal eigenvalue as the NTK eigenvectors corresponding to the principal eigenvalue are learned quicker due to spectral bias [10, 12, 59, 64]. This motivates the use of the principal eigenvalue λ_1^l in our client-specific layer importance score, as it represents the maximum alignment of each layer's parameter space with the client's data distribution. This provides a principled basis for prioritizing these layers.

For a step of gradient descent, the loss reduction can be characterized by the directional derivative of the loss:

$$\Delta \mathfrak{L} \overset{(i)}{=} \lim_{\epsilon \to 0} \frac{\mathfrak{L}(\theta + \epsilon \nabla_\theta \mathfrak{L}(\theta)) - \mathfrak{L}(\theta)}{\epsilon} \overset{(ii)}{\approx} \nabla_\theta \mathfrak{L}(\theta)^T \nabla_\theta \mathfrak{L}(\theta)$$
$$\overset{(iii)}{=} \nabla_Z \mathfrak{L}(\theta)^T (\nabla_\theta F(\theta)^T \nabla_\theta F(\theta)) \nabla_Z \mathfrak{L}(\theta)$$
$$\overset{(iv)}{=} \nabla_Z \mathfrak{L}(\theta)^T \left(\sum_{l=1}^L \Theta^l \right) \nabla_Z \mathfrak{L}(\theta) \overset{(v)}{=} \sum_{l=1}^L \sum_{j=1}^{nk} \lambda_j^l \left((u_j^l)^T Y \right)^2$$
$$\overset{(vi)}{\approx} \sum_{l=1}^L \lambda_1^l \left((u_1^l)^T Y \right)^2 \qquad (12)$$

where (i) follows the definition of the directional derivative; (ii) follows the first-order Taylor expansion; (iii) applies the chain rule of derivatives; (iv) follows from Eq. (8); and (v) follows the eigen-decomposition of the layerwise NTK under the assumption of squared error loss. Assuming that the true labels align well with the top eigenvectors as
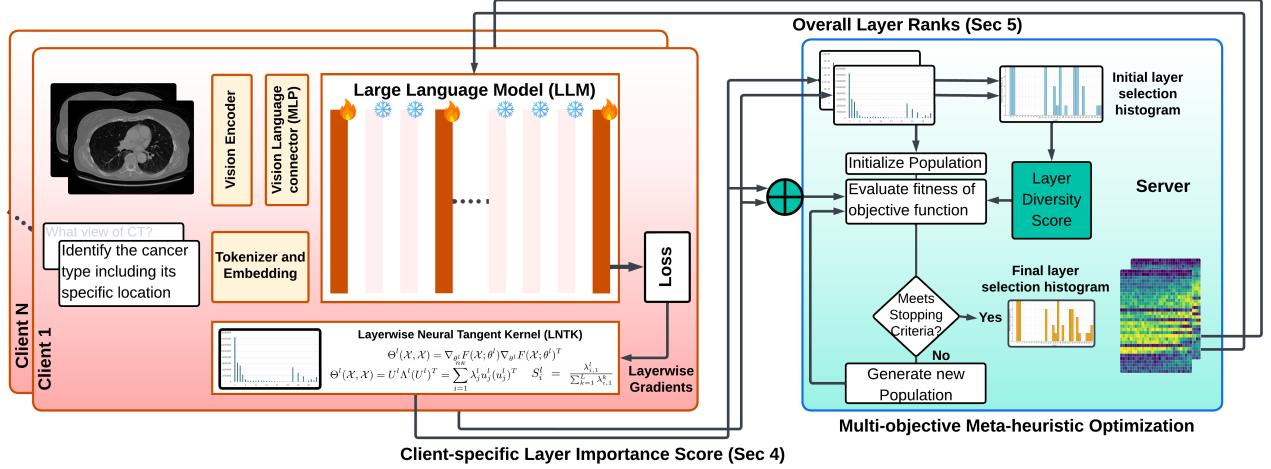
Figure 4. Overview of our layer selection strategy, F^3OCUS. Each client sends layer importance scores based on the principal eigenvalue of LNTK to the server. The server refines client-specific layer selection by maximizing the cumulative client-specific importance scores while simultaneously minimizing the variance of the histogram of layer selections across clients. It sends the revised layer ranks back.
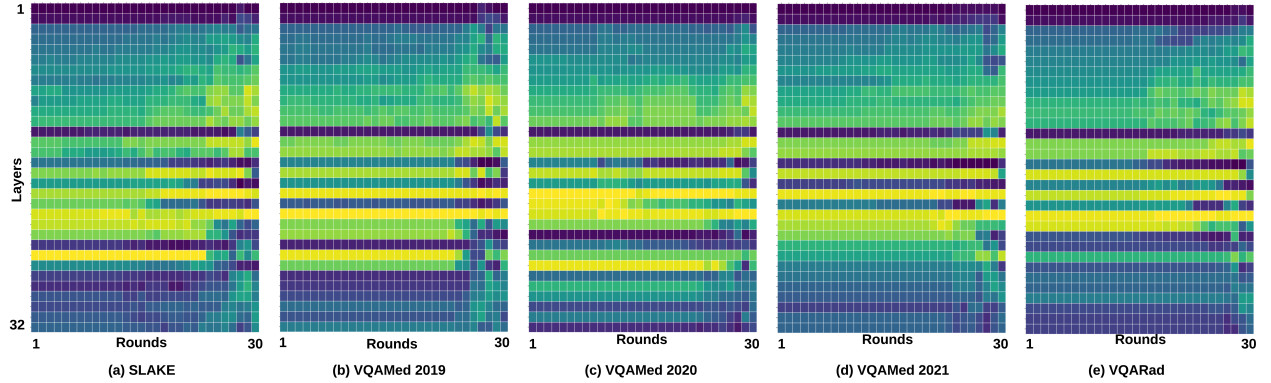

Figure 5. Visualization of layer ranks of LLaVA-1.5 across rounds in different clients based on LNTK. Darker color implies higher rank.

discussed earlier, *i.e.*, $\left((u_j^l)^T Y\right)^2$ is large for large λ_j^l, directional derivative of the loss function can be regarded as closely related to the eigenspectrum of the layerwise NTKs. Specifically, (vi) suggests that layers with higher principal eigenvalues contribute more significantly to loss reduction during training. Overall, Eq. 12 suggests that the loss decreases more rapidly along the eigenspaces corresponding to larger LNTK eigenvalues. Given that the principal eigenvalue λ_1^l vary across layers as seen in Fig. 3, we propose to selectively fine-tune layers with larger λ_1^l to achieve efficient learning with limited computational resources.

Therefore, we define the **client-specific layer importance score** $S_i^l = \frac{\lambda_{i,1}^l}{\sum_{k=1}^{L} \lambda_{i,1}^k}$ where the sum in the denominator normalizes the principal eigenvalue across all layers, ensuring that S_i^l captures the relative importance of each layer for client i in terms of its contribution to the model's predictive capacity for that client's data distribution. This formulation prioritizes layers whose NTK principal eigen-

values dominate, indicating strong client-specific parameter alignment (see Figs. 3 & 5). **See Algorithm in Suppl. §A.**

4.2. Convergence Analysis of LNTK

We begin with some necessary assumptions following previous works [34, 73] and then introduce a set of assumptions to analyze the impact of the layers selected using LNTK:

Assumption 1: (γ-Smoothness) There exists a constant $\gamma > 0$ such that for any $\theta, \phi \in \mathbb{R}^p$:

$$\|\nabla F_i(\theta) - \nabla F_i(\phi)\|_2 \leq \gamma \|\theta - \phi\|_2, \quad \forall i \in \mathcal{N}. \tag{13}$$

Assumption 2: (Unbiased and variance-bounded stochastic gradient) The layerwise stochastic gradient $G_{i,l}(\theta_t; B_{i,t})$ computed on a randomly sampled data batch $B_{i,t}$ serves as an unbiased estimate of the layerwise full-batch gradient:

$$\mathbb{E}_{B_{i,t}}[G_{i,l}(\theta_t; B_{i,t})] = \nabla F_{i,l}(\theta_t). \tag{14}$$

Besides, there exist constants $\sigma_l > 0, \forall l \in \mathcal{L}$ such that $\mathbb{E}_{B_{i,t}} \| G_i^l(\theta_t; B_{i,t}) - \nabla F_i^l(\theta_t) \|^2 \leq \sigma_l^2, \forall i \in \mathcal{N}$ and $\sum_{l \in \mathcal{L}} \sigma_l^2 \leq \sigma^2$.

Assumption 3: (Gradient Diversity) The non-IID client data distribution causes diverse gradients. There exist constants $\kappa_l > 0, \forall l \in \mathcal{L}$ such that:

$$\mathbb{E}_{B_{i,t}}[\|\nabla F(\theta_t) - \nabla F_i^l(\theta_t; B_{i,t})\|^2] \leq \kappa_l^2, \forall i \in \mathcal{N}. \quad (15)$$

In contrast to the theoretical analysis for standard FL settings, our LNTK-based fine-tuning introduces three additional challenges: *(i)* Each client only updates a subset of layers. Hence, the aggregated gradient is no longer an unbiased estimate of the local gradient $\nabla F_i(\theta_t)$, *i.e.*, $\sum_{l \in \mathcal{L}_t} \nabla F_i^l(\theta_t) \neq \nabla F_i(\theta_t)$ where equality holds only if all layers are selected. *(ii)* LNTK-based layer selection may vary across clients as seen in Fig. 5. The aggregated gradient of the selected layers is not equal to the gradient computed based on the global loss function *i.e.*, $\sum_{i \in \mathcal{S}^t} \sum_{l \in \mathcal{L}_t} \alpha_{i,t} \nabla_l F_i(\theta_t) \neq \sum_{l \in \mathcal{L}_t} \nabla_l F(\theta_t)$, where equality holds only if all clients select the same layers.
(iii) The gradient magnitudes in *(i-ii)* vary across epochs.

In order to relate the aggregated and target gradient, we define a proxy layerwise loss $\psi_{i,l}$ optimized by clients as:

$$\psi_i^l(\theta_t) \triangleq \sum_{i \in \mathcal{S}_t} m_{i,t}^l \alpha_{i,t} F_i^l(\theta_t), \quad \text{s.t } \nabla_l \psi_i^l(\theta_t) = \delta_t \quad (16)$$

Given assumptions 1-3, we formulate the convergence as:
Theorem 1 (Convergence of LNTK-based layer selection):

$$\min_{t \in [T]} \mathbb{E}\left[\|\nabla F(\theta_t)\|_2^2\right] \leq \frac{2}{(\eta - \gamma \eta^2)T}\left[\left[F(\theta^0) - F(\theta^*)\right]\right.$$
$$+ \gamma(\eta\sigma)^2 T + \sum_{t=1}^{T}\left(\eta + \frac{1}{2\gamma} - \gamma\eta^2\right)\left(\mathbb{E}\left[\left\|\sum_{\ell \notin \mathcal{L}_t} \nabla_\ell F(\theta_t)\right\|^2\right]\right.$$
$$\left.\left.+ \sum_{\ell \in \mathcal{L}_t} \sum_{i \in \mathcal{N}} \alpha_{i,t}(1 - m_{i,t}^l)^2 k_l^2\right)\right] \quad \text{s.t } \theta^* = \arg\min_{\theta \in \mathbb{R}^p} F(\theta)$$
$$(17)$$

Remark 1: With commonly chosen $\eta = O\left(\frac{1}{\sqrt{T}}\right)$, RHS of (17) the last term $\to 0$ as $T \to \infty$. So, LNTK-based PEFT-FL converges to a small neighbourhood of a stationary point of standard FL, maintaining a non-zero error floor. **See Suppl. §B for complete proof and discussions.**

5. Server-level Overall Layer Importance

5.1. Theoretical Motivation

To explicitly examine the impact of potential noise introduced by LNTK-based layer selection as well the variation of selection count across clients, we reformulate the convergence in Theorem 2 leveraging two additional assumptions:

Assumption 4: (Bounded stochastic gradient) The expected squared norm of stochastic gradients is bounded uniformly, *i.e.*, for constant $\sigma_g > 0$ and any i, t:

$$\mathbb{E}_{B_{i,t}}[\|G_i(\theta_t; B_{i,t})\|^2] \leq \sigma_g^2. \quad (18)$$

Assumption 5: (Normalized Layer Selection Noise Bound) There exist some $\xi^2 \in [0, 1)$ and any t, i, the normalized layer selection noise due to LNTK is bounded by:

$$\frac{\|\theta_t - \hat{\theta}_{t,i}\|^2}{\|\theta_t\|^2} \leq \xi^2 \quad (19)$$

where $\hat{\theta}_{t,i}$ denotes LNTK-based client-specific layers.
Theorem 2 (Impact of layer selection-based noise ξ and variance of selection count s_d^2 on LNTK convergence):

$$\min_{t \in [T]} \mathbb{E}\left[\|\nabla F(\theta_t)\|_2^2\right] \leq \frac{2}{(\eta - 3\gamma\eta^2)T}\left[F(\theta^0) - F(\theta^*)\right.$$
$$+ \sum_{t=1}^{T} \frac{\eta \xi^2 \gamma^2 N s_d}{2}(1 + 3\eta\gamma)\mathbb{E}\left[\left\|\sum_{t=1}^{T} \nabla_\ell F(\theta_t)\right\|^2\right]$$
$$\left. + \frac{\gamma\eta^2 N T s_d}{2}\left(\eta\gamma\sigma_g^2(1 + 3\gamma) + 3\sigma^2 s_d\right)\right] \text{s.t} \quad \theta^* = \arg\min_{\theta \in \mathbb{R}^p} F(\theta)$$
$$(20)$$

Remark 2: With $\eta \leq \min\{\frac{1}{\sqrt{T}}, \frac{1}{6\gamma}\}$, model converges to a neighborhood of a stationary point of FL with a small gap due to layer selection-based noise ξ and variance of selection count s_d over clients. This motivates us to jointly minimize the influence of ξ and s_d for better convergence.

5.2. Multi-objective Optimization

Motivated by this, we refine the selected layers on server (see Fig. 6) to achieve two primary objectives (see Eq. 21): maximizing the cumulative client-specific importance scores based on LNTK and minimizing the variance of layer selection histogram (see Fig. 7) to encourage more balanced usage of each layer over clients. Let n_l represent the number of clients that select layer l, with $\bar{n} = \frac{1}{L}\sum_{l=1}^{L} n_l$ as the mean count of layer usage. (**See Suppl. §A for more details.**) The joint optimization problem is formulated as:

$$\begin{cases} \max & \sum_{i=1}^{\mathcal{N}} \sum_{l=1}^{L} S_i^l \\ \min & \frac{1}{L}\sum_{l=1}^{L}(n_l - \bar{n})^2 \end{cases} \text{s.t:} \sum_{l \in \mathcal{L}_i} m_i^l \leq L_{i,\max}, \quad \forall i \in \mathcal{N}$$
$$(21)$$

The latter objective prevents over-reliance on specific layers even if they have high importance scores thereby increasing diversity in layer selection across clients. The constraint incorporates client-specific computational budget $L_{i,\max}$.

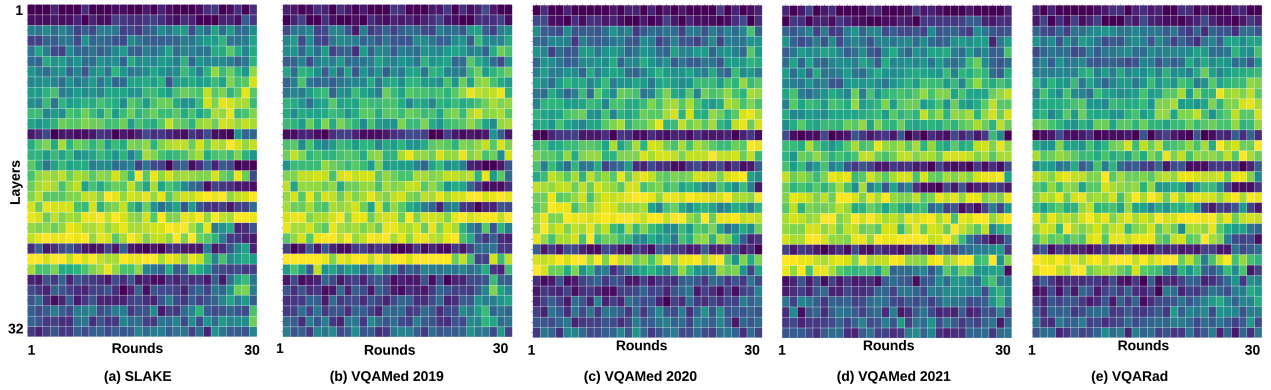Traditional optimization methods struggle to optimize these two conflicting objectives. Neural networks cannot be

Figure 6. Visualization of refined layer ranks of LLaVA-1.5 based on F^3OCUS. Comparing it with Fig. 5 shows that the server-level meta-heuristic optimization refines the client-level layer ranks by increasing inter-client layer diversity at every round.
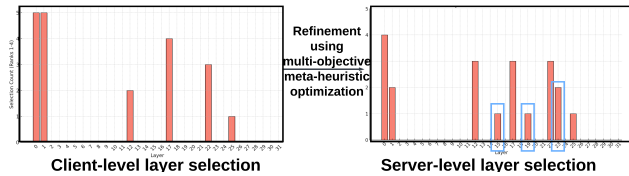

Figure 7. Layer selection histogram shows the impact of server-level optimization. It encourages more layers to participate (see blue-marked areas) by maximizing layer-selection diversity *i.e.*, reducing the variance of the selection count (vertical axis).

employed to optimize due to absence of data on server. Besides, the number of possible configurations is particularly high due to the large number of layers in foundation models. Since this problem involves multiple objectives, there is no "best" solution but rather a set of optimal trade-offs (the Pareto front). Meta-heuristic algorithms are well-suited to explore such complex, high-dimensional solution spaces in absence of training data by balancing exploration and exploitation. To this end, we carefully select and investigate 5 meta-heuristic algorithms spanning all 3 algorithm categories: evolutionary, physics-based, and swarm-based. **See Suppl. §A for detailed description and pseudo-code.**

5.3. Meta-heuristic algorithms

Each of the following algorithms aim to maximize client-specific importance while ensuring balanced layer utilization across clients based on their underlying principles:

(1) **Non-Dominated Sorting Genetic Algorithm (NSGA):** We use NSGA [20] to iteratively evolve a population of layer selections. We initialize population based on client-specific importance scores while incorporating probability-based sampling for broader search space coverage. This guided randomness helps balance **exploration** (diversifying choices) and **exploitation** (prioritizing high-importance layers). Genetic operations like **crossover** and **mutation** generate new solutions, while **non-dominated sorting** and **crowding distance** ensure diversity on the Pareto Front.

(2) **Artificial Bee Colony (ABC) [4]:** Each bee represents a potential layer selection for the clients. The optimization proceeds in three phases: **Employed bees** exploit local solutions, adjusting layer assignments based on importance scores and diversity, occasionally accepting worse solutions to escape local optima. **Onlooker bees** then select solutions based on a probability weighted by importance and diversity, while **Scout bees** abandon unproductive solutions, replacing them with randomly generated ones to promote exploration. Non-dominated solutions are stored in a Pareto archive, which guides refinement over iterations.

(3) **Ant Colony Optimization (ACO) [21]:** Each ant represents a candidate layer selection, constructing paths influenced by **pheromone trails** (which reinforce successful layer choices from previous iterations) and **importance scores** (which guide ants toward layers that are likely beneficial based on client-specific requirements). The Pareto archive preserves non-dominated solutions. Pheromone trails are then updated, with evaporation to prevent stale paths and additional pheromone deposits on layers selected, thereby encouraging their selection in subsequent iterations.

(4) **Simulated Annealing (SA):** SA [71] starts with a high-temperature, randomly initialized solution, gradually exploring optimal layer selections by cooling over iterations. It accepts new configurations if it offers higher importance or lower variance based on Eq. 21. If the new configuration is less optimal, it may still be accepted based on a probability that decreases with the temperature allowing SA to avoid being trapped in local optima. As the temperature cools, SA gradually refines the search, focusing on fine-tuning layer assignments that respect both client-specific importance and a balanced distribution of layer usage.

(5) **Multi-Objective Particle Swarm Optimization (MOPSO) [18]:** Each particle in the swarm represents a candidate layer assignment, initialized with client-specific

importance scores to guide the selection of important layers. Randomized probability-based sampling is used to ensure diverse initial positions, promoting exploration of the solution space. Each particle updates its **velocity** and **position** by balancing three influences: **inertia** (maintaining its current layer selection), **a cognitive component** (best individual solution), and **a social component** (globally optimal solution).

6. Experiments and Results

6.1. FL settings, Datasets and Tasks

We evaluate our performance for fine-tuning selected (i) layers, and (ii) adapters [29] with 4 VLMs of varying size and architecture, *viz.*, ViLT [35], ALBEF [45], LlAVA-1.5 [51], and BLIP-2 [46], for 3 FL task settings: (a) Visual Question Answering, (b) Image and Text-based Disease Classification, (c) Heterogeneous tasks combining (a), (b).

(a) Visual Question Answering: We consider **3** scenarios with data of varying sizes, class counts, and complexity:

(i) **Task 1 (with Domain gap):** **Five-client setting** with SLAKE [50], VQA-RAD [37], VQA-Med 2019 [6], VQA-Med 2020 [1], and VQA-Med 2021 [7].

(ii) **Task 2 (with Modality gap):** **Modality specific 8-client setting** with CT, Ultrasound, Dermatoscopy, Fundus, Histology, Microscopy, OCT, and X-Ray clients.

(iii) **Task 3 (with Modality gap):** **Modality specific 9-client setting** with our Ultra-MedVQA dataset **(see Fig. 8)**.

(b) Image and text-based multi-label disease classification: We consider **2** FL settings [62] with Dirichlet coefficient $\gamma = 0.5$ for Chest X-Ray and Radiology report-based multi-label disease detection (with 15 classes).

(i) **Task 4 (with label shift):** **4 client-scenario** with Open-I

(ii) **Task 5 (w/ label shift):** **10 client scenario** with MIMIC.

(c) Heterogeneous tasks: We consider **Task 6 (with task heterogeneity)** combining three Visual Question answering clients, *viz.*, SLAKE, VQA-RAD, VQA-Med 2019, and two disease-classification clients, *viz.*, Open-I and MIMIC.

Device Heterogeneity: In Tab. 2 and 5, to simulate varying resource constraints among clients, we adjust the number of trainable layers across different tasks. For Tasks 1 and 6, 6 layers are finetuned for 2 clients, 4 layers for another 2 clients, and 2 layers for the remaining client. For Task 2, 6 layers are finetuned for 3 clients, 4 layers for 3 clients, and 2 layers for the last 2 clients. For Task 3, 2 layers are finetuned for 3 clients, 4 layers for another 3 clients and 6 layers for the last 3 clients. For Task 4, 6 layers are finetuned for 1 client, 4 layers for another client, and 2 layers for the remaining 2 clients. For Task 5, 6 layers are finetuned for 3 clients, 4 layers for 1 client, and 2 layers for the last client.

See Suppl. §C for dataset and implementation details

6.2. Performance comparison with State-of-the-arts

We compare F^3OCUS with **28 SOTA** methods:

(i) Tab. 3 shows comparison with **5 SOTA PEFT baselines**, *viz.*, LayerNorm Tuning (LN) [5], LoRA [30], Bias Tuning [11], Prompt Tuning [25], and FedDAT [14] in terms of communication (MBits), Computation (GFLOPs), total number of trainable parameters (Millions) and accuracy in each client. F^3OCUS is observed to outperform all PEFTs except adapters [29] and FedDAT which finetune all adapters whereas F^3OCUS finetunes only selected 4 adapter layers in each client leading to reduced communication (9.7 MBits) and computational needs (80.6 GFLOPs).

(ii) In Tab. 6, F^3OCUS is seen to consistently outperform **12 SOTA Personalized FL baselines** *viz.* perFedavg [23], MetaFed [17], FedPAC [75], FedAS [78], FLUTE [52], FedALA [81], FedProto [68], FedRod [15], FedAP [53], FedFomo [85], FedRep [19], and Fedper [3] for 5 tasks.

(iii) We adapt 7 **SOTA Pruning baselines** *viz.* Federated Drop-out [74], Magnitude [26], FishMask [66], GradFlow [54], GraSP [72], SNIP [40], and Synflow [69] in our context and compare with proposed method in Tabs. 2 and 5. LNTK surpasses the performance of the closest SOTA pruning method by **2.11%** and **2.30%** while F^3OCUS outperforms it by **5.35%** and **5.33%** respectively for homogeneous and heterogeneous device settings over all architectures.

(iv) We also compare with **4 SOTA Layer Selection baselines** *viz.* Adapter-drop (denoted as 'last') [61], RGN [42], Fedselect [67], and SPT [27] (see Tabs. 2, 5). From Table 2, we observe that LNTK outperforms the closest SOTA method by **2.08%** and **2.17%** for homogeneous and heterogeneous resource settings respectively. F^3OCUS further improves performance over LNTK by **3.24%** and **3.03%**.

6.3. Other Experimental Results

We plot the loss curves of LNTK and F^3OCUS and compare them with several pruning methods in **Fig. 2**, which demonstrates the impact of our server-level optimization on faster convergence. We also visualize the principal eigenvalue magnitudes of all 32 layers of LLaVA across different clients at the beginning of a round for Task 1 in **Fig. 3** and show the layer ranks over all rounds in **Fig. 5**. Consequently, the effect of server-level optimization on overall layer selections is shown in **Fig. 6** using relative layer ranks and in **Fig. 7** using the layer selection histogram. In **Fig. 9**, we motivate the current work by revealing that, contrary to common belief, fine-tuning the last 'K' layers is only as effective as fine-tuning random 'K' layers. **Table 4** shows the comparable performance of different meta-heuristic algorithms for all clients in Task 2. For the 'microscopy' client in the same task, we present t-SNE feature visualizations in **Fig. 10** for (a) Federated Dropout (labeled random), (b) LNTK, and (c) F^3OCUS, highlighting the striking improvement in generating distinctive feature representations.
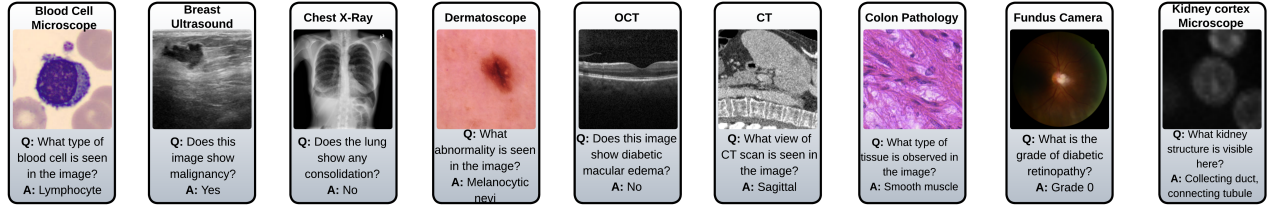
Figure 8. Sample VQA triplets of 9 modality-specific medical clients from Ultra-MedVQA (**Task 3**)

Table 2. Performance comparison on VLM adapter layer selection in terms of accuracy for Tasks 1-3 and F1-score for Tasks 4-6

| Fine-tuning	Task 1			Task 2			Task 3			Task 4			Task 5			Task 6			Mean Score		
	ViLT	LLAVA	BLIP	ViLT	LLAVA	BLIP	ViLT	LLAVA	BLIP	ViLT	LLAVA	BLIP	ViLT	LLAVA	BLIP	ViLT	LLAVA	BLIP	ViLT	LLAVA	BLIP
All adapters	43.04	40.02	43.36	82.46	79.70	79.03	78.55	75.19	76.40	63.05	76.89	71.05	65.68	77.93	76.30	85.83	88.02	89.26	69.77	72.96	72.57
	Homogeneous resources across clients (L=4 for all clients)																				
FD [74]	33.54	33.31	34.15	73.94	68.84	68.78	70.36	67.04	68.54	52.82	67.78	60.21	56.20	67.99	66.53	76.90	79.05	80.36	60.63	64.00	63.10
Last [61]	33.91	33.04	35.19	70.53	65.63	66.92	68.32	65.03	66.59	54.40	65.94	58.45	57.77	66.05	64.20	77.62	79.51	79.96	60.42	62.53	61.88
Magnitude [26]	31.60	32.40	30.26	70.32	67.35	67.67	69.18	68.73	69.02	54.33	66.59	61.80	56.01	66.90	64.98	77.14	80.26	80.44	59.76	63.71	62.36
FishMask [66]	37.45	35.34	37.77	75.65	72.37	71.38	71.99	71.63	72.10	56.02	72.04	65.35	59.20	71.86	70.22	79.98	83.03	82.32	63.38	67.71	66.52
GradFlow [54]	36.03	34.29	38.35	74.81	72.65	72.58	72.29	69.88	71.09	56.38	71.19	64.98	59.82	71.60	70.13	80.33	82.89	82.56	63.28	67.08	66.61
GraSP [72]	35.46	34.90	38.88	75.03	72.03	71.74	72.03	71.39	71.76	55.83	70.73	65.43	60.00	70.07	69.20	81.02	83.48	82.19	63.23	67.10	66.53
SNIP [40]	31.26	32.73	35.36	73.96	69.40	70.15	72.16	67.04	68.76	54.21	66.07	60.39	58.09	67.24	66.92	78.20	80.34	81.13	61.31	63.80	63.78
RGN [42]	32.71	32.52	34.81	73.60	69.94	70.55	70.88	68.75	69.73	56.40	67.25	61.32	57.54	68.64	68.39	76.79	78.05	80.09	61.32	64.19	64.15
Synflow [69]	35.68	35.38	37.89	75.26	72.33	73.25	72.49	71.36	71.63	56.11	71.67	64.28	59.27	70.17	71.32	80.35	79.09	81.90	63.19	66.67	66.71
Fedselect [67]	36.80	34.48	38.88	74.29	70.49	71.63	71.29	70.52	70.06	55.83	70.86	65.08	58.53	71.33	72.02	79.39	83.22	83.00	62.69	66.82	66.78
SPT [27]	35.59	34.40	38.53	75.50	72.16	71.32	72.58	70.78	71.56	56.74	71.98	65.71	59.71	71.45	71.35	80.13	83.89	82.99	63.38	67.44	66.91
LNTK (ours)	39.74	36.80	40.43	77.54	74.64	74.49	74.01	72.68	73.93	58.07	73.06	67.80	61.50	73.00	73.43	82.04	85.79	84.84	65.48	69.33	69.15
F^3OCUS (ours)	**42.41**	39.85	43.04	81.31	78.78	78.70	77.86	75.01	76.45	62.51	76.70	70.35	64.62	77.26	76.14	85.28	87.53	88.30	69.00	72.52	72.16
	Heterogeneous resources across clients																				
FD [74]	32.65	33.54	34.04	73.74	69.36	68.16	70.27	66.73	67.81	52.18	67.51	60.48	55.56	67.71	66.16	76.85	78.57	79.54	60.21	63.90	62.70
Last [61]	33.65	33.80	35.30	70.90	65.81	66.97	68.22	65.92	66.31	54.89	66.35	58.43	57.91	65.47	64.75	77.86	78.80	80.12	60.57	62.69	61.98
Magnitude [26]	32.04	32.54	30.81	69.84	67.00	67.53	68.54	68.48	68.57	53.83	66.19	61.46	56.12	66.30	65.11	77.68	80.48	80.78	59.68	63.50	62.38
FishMask [66]	37.43	35.73	37.78	75.60	72.01	71.70	71.78	71.34	71.45	56.58	72.08	65.17	59.40	72.25	70.37	80.49	82.66	82.01	63.55	67.68	66.41
GradFlow [54]	35.17	34.86	38.43	75.41	73.16	71.99	72.45	70.40	71.20	56.33	70.91	65.17	59.44	71.48	70.19	80.66	83.39	82.96	63.24	67.37	66.66
GraSP [72]	36.11	35.20	38.68	74.99	72.38	70.99	71.54	71.54	71.98	55.50	71.12	65.24	59.50	69.63	69.17	81.85	82.63	81.48	63.25	67.06	66.26
SNIP [40]	30.53	33.39	36.24	73.96	68.70	70.33	72.00	66.63	68.03	54.02	66.76	60.09	58.82	67.15	66.90	78.01	79.66	81.14	61.22	63.72	63.79
RGN [42]	31.82	32.64	35.14	73.74	70.12	70.52	70.49	69.04	69.13	56.02	67.68	61.42	58.22	69.21	68.50	77.04	78.52	79.75	61.22	64.54	64.08
Synflow [69]	35.80	36.02	38.33	75.70	72.17	72.57	72.63	71.47	70.97	57.02	72.26	64.49	59.23	70.09	70.65	80.40	78.53	82.78	63.46	66.76	66.63
Fedselect [67]	36.59	34.21	39.00	74.85	69.71	70.94	71.12	70.77	69.85	55.71	70.70	64.35	58.07	71.51	71.79	79.26	83.42	83.45	62.60	66.72	66.56
SPT [27]	35.35	34.72	38.58	75.34	72.84	71.82	72.92	70.87	72.10	56.23	72.65	65.38	59.38	72.05	71.20	80.41	83.82	82.44	63.27	67.82	66.92
LNTK (ours)	39.24	37.56	40.02	77.59	74.55	74.96	73.14	73.37	74.68	58.12	73.40	67.50	62.32	73.34	73.65	82.44	86.32	84.96	65.48	69.76	69.29
F^3OCUS (ours)	41.80	40.06	43.42	81.85	77.83	79.13	77.16	75.04	76.33	62.18	76.69	71.08	64.42	77.59	75.73	85.28	87.56	88.45	68.78	72.46	72.36
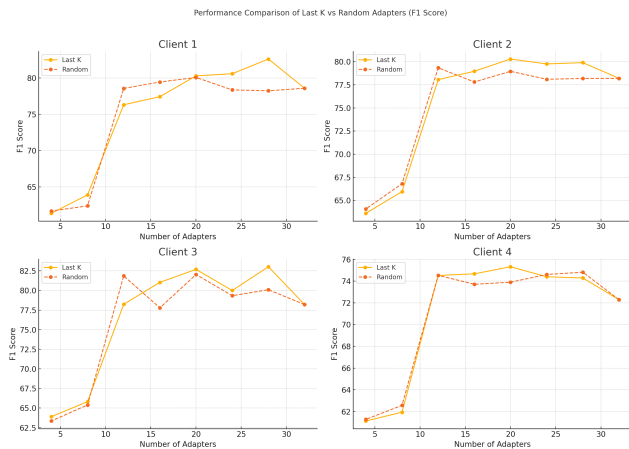
Figure 9. Performance of last 'K' and random 'K' adapters for 32-layered LLaVA-1.5-7b on **Task 4**

Table 3. Comparison with other PEFTs on **Task 1** using **ALBEF**

Method	MBit	GFLOP	Param(M)	SLAKE	VM2019	VM2020	VM2021	VR	Overall
Full	3915.2	156.5	122.35	77.45	67.25	15.06	22.00	41.52	46.92
Adap (all)	28.8	85.2	0.90	72.82	64.45	11.56	21.00	38.35	43.17
FedDAT	86.1	86.3	2.69	72.79	63.58	12.46	23.00	38.91	43.93
LN	5.8	84.7	0.18	69.53	62.22	10.59	22.00	36.89	41.30
LoRA	19.5	84.6	0.61	57.73	60.18	4.59	15.00	31.16	35.09
Bias	3.5	84.7	0.11	68.25	55.61	11.17	17.00	35.47	39.54
PromptFL	19.2	85.0	0.60	65.63	57.56	4.78	15.00	40.26	36.65
F^3OCUS	9.7	80.6	0.30	74.69	60.05	12.84	24.00	42.30	42.78

Table 4. Comparison of meta-heuristic methods (Task 2)

Finetune	C1	C2	C3	C4	C5	C6	C7	C8	Overall
	(CT)	(US)	(OCT)	(Fundus)	(Micro.)	(Hist.)	(Derma.)	(XRay)	
NSGA	88.67	**79.41**	78.29	83.48	70.68	88.49	**67.69**	73.93	**78.78**
ABC	**91.33**	74.51	77.71	85.71	**72.73**	88.70	62.31	**76.55**	78.70
ACO	86.67	78.10	**78.86**	83.48	70.68	88.08	66.92	76.00	78.60
SA	88.67	72.59	70.86	**85.93**	71.09	**89.45**	66.62	76.48	77.71
MOPSO	86.18	77.31	78.83	84.53	71.18	87.58	65.49	75.97	78.38

See Suppl. §D for more results and detailed discussions.

Table 5. Performance comparison on VLM layer selection with heterogeneous resources across clients

Fine-tuning	Task 1		Task 2		Task 3		Task 4		Task 5		Task 6	
	ViLT	BLIP	ViLT	BLIP	ViLT	BLIP	ViLT	BLIP	ViLT	BLIP	ViLT	BLIP
FD [74]	31.91	33.07	75.75	70.03	72.84	70.13	50.25	58.12	56.80	68.10	77.65	82.70
Last [61]	32.75	34.31	76.65	68.35	72.63	68.56	53.77	56.46	59.07	66.25	80.75	81.70
Magnitude [26]	31.35	30.96	73.26	69.18	70.88	71.02	52.17	58.46	58.25	67.04	77.51	82.27
FishMask [66]	36.35	36.82	77.71	73.56	74.60	73.61	54.35	63.08	61.10	73.39	81.90	83.09
GradFlow [54]	36.20	37.29	77.09	74.06	74.82	73.90	54.18	62.58	60.70	71.76	81.22	82.24
GraSP [72]	35.36	37.87	76.90	73.00	73.80	74.83	53.44	62.68	60.91	70.85	82.03	82.54
SNIP [40]	29.65	35.23	75.59	73.88	74.37	72.14	51.91	58.04	62.04	68.85	79.25	82.38
RGN [42]	32.89	36.21	75.34	72.35	72.76	71.59	53.80	62.16	59.58	70.23	77.95	81.14
Synflow [69]	34.99	37.39	77.95	74.05	74.81	73.79	55.09	62.08	60.97	72.10	81.30	83.65
Fedselect [67]	35.79	38.00	76.66	72.80	73.45	72.60	53.55	61.87	59.34	71.63	80.29	84.10
SPT [27]	34.33	37.78	77.03	73.66	75.18	74.80	54.18	63.03	60.60	72.68	81.53	83.97
LNTK	37.32	39.22	79.15	76.47	75.44	76.99	55.81	65.40	64.12	75.26	83.66	86.20
F^3OCUS	**40.85**	**42.37**	**84.25**	**80.46**	**79.65**	**78.95**	**60.29**	**69.79**	**65.86**	**78.94**	**86.40**	**89.69**

Table 6. Comparison with SOTA personalized FL (L=4)

Task	perFedavg	MetaFed	FedPAC	FedAS	FLUTE	FedALA	FedProto	FedRod	FedAP	FedFomo	FedRep	Fedper	F^3OCUS
1	33.87	35.42	36.17	36.46	30.83	35.50	35.46	36.23	36.84	35.44	35.30	36.14	**42.41**
2	71.61	75.46	76.29	76.51	62.33	74.56	74.98	77.65	77.42	75.13	75.49	75.93	**81.31**
4	54.56	57.26	57.53	58.78	44.84	57.18	57.00	59.35	59.49	57.05	58.36	58.08	**62.51**
5	57.64	59.15	58.73	59.17	47.88	57.42	57.38	58.77	60.44	58.34	57.01	57.58	**64.62**
6	73.28	76.27	78.17	78.51	63.19	75.88	77.04	76.10	76.33	75.66	76.55	76.76	**85.28**

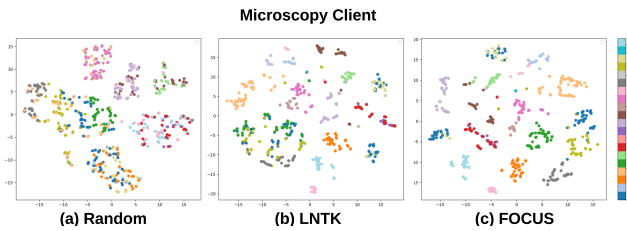

Figure 10. t-SNE feature visualization for Client 6 of Task 2 (with 26 classes) shows greater separability for F^3OCUS.

7. Conclusion

We presented F^3OCUS, a novel and theoretically grounded approach for federated fine-tuning of Vision-Language foundation models in client-specific resource-constrained settings. F^3OCUS effectively balances individual client requirements with collective layer diversity thereby improving model convergence and performance accuracy. Our server-level multi-objective meta-heuristic optimization scheme does not require any data on server and can be easily combined with any existing layer selection or pruning algorithms. Additionally, we released **Ultra-MedVQA**, the largest medical VQA dataset, covering 12 anatomies, for supporting further VLM research. Experimental results demonstrate that F^3OCUS achieves supe-

rior performance across multiple vision-language tasks and models, providing a practical solution for fine-tuning large foundation models in decentralized environments. **Our code and dataset will be made available upon acceptance.**

References

[1] Abeed S. Ben Abacha, Vivek V. Datla, Sadid A. Hasan, Dina Demner-Fushman, and Henning Müller. Overview of the vqa-med task at imageclef 2020: Visual question answering and generation in the medical domain. In *CLEF 2020 Working Notes*. 8

[2] Durmus Alp Emre Acar, Yue Zhao, Ramon Matas Navarro, Matthew Mattina, Paul N Whatmough, and Venkatesh Saligrama. Federated learning based on dynamic regularization. *arXiv preprint arXiv:2111.04263*, 2021. 1, 3

[3] Manoj Ghuhan Arivazhagan, Vinay Aggarwal, Aaditya Kumar Singh, and Sunav Choudhary. Federated learning with personalization layers. *arXiv preprint arXiv:1912.00818*, 2019. 8

[4] Jagdish Chand Bansal, Harish Sharma, and Shimpi Singh Jadon. Artificial bee colony algorithm: a survey. *International Journal of Advanced Intelligence Paradigms*, 5(1-2): 123–159, 2013. 7

[5] Samyadeep Basu, Daniela Massiceti, Shell Xu Hu, and Soheil Feizi. Strong baselines for parameter efficient few-shot fine-tuning. *arXiv preprint arXiv:2304.01917*. 8

[6] Asma Ben Abacha, Sadid A Hasan, Vivek V Datla,

Dina Demner-Fushman, and Henning Müller. Vqa-med: Overview of the medical visual question answering task at imageclef 2019. In *Proceedings of CLEF (Conference and Labs of the Evaluation Forum) 2019 Working Notes*, 2019. 8

[7] Asma Ben Abacha, Mourad Sarrouti, Dina Demner-Fushman, Sadid A Hasan, and Henning Müller. Overview of the vqa-med task at imageclef 2021: Visual question answering and generation in the medical domain. In *Proceedings of the CLEF 2021 Conference and Labs of the Evaluation Forum-working notes*, 2021. 8

[8] Elad Ben Zaken, Yoav Goldberg, and Shauli Ravfogel. Bit-Fit: Simple parameter-efficient fine-tuning for transformer-based masked language-models. In *Proceedings of the Association for Computational Linguistics (Volume 2: Short Papers)*, pages 1–9, Dublin, Ireland, 2022. 2

[9] Florian Bordes, Richard Yuanzhe Pang, Anurag Ajay, Alexander C. Li, Adrien Bardes, Suzanne Petryk, Oscar Mañas, Zhiqiu Lin, Anas Mahmoud, Bargav Jayaraman, Mark Ibrahim, Melissa Hall, Yunyang Xiong, Jonathan Lebensold, Candace Ross, Srihari Jayakumar, Chuan Guo, Diane Bouchacourt, Haider Al-Tahan, Karthik Padthe, Vasu Sharma, Hu Xu, Xiaoqing Ellen Tan, Megan Richards, Samuel Lavoie, Pietro Astolfi, Reyhane Askari Hemmat, Jun Chen, Kushal Tirumala, Rim Assouel, Mazda Moayeri, Arjang Talattof, Kamalika Chaudhuri, Zechun Liu, Xilun Chen, Quentin Garrido, Karen Ullrich, Aishwarya Agrawal, Kate Saenko, Asli Celikyilmaz, and Vikas Chandra. An introduction to vision-language modeling, 2024. 1

[10] Benjamin Bowman. A brief introduction to the neural tangent kernel. 2023. 4

[11] Han Cai, Chuang Gan, Ligeng Zhu, and Song Han. Tinytl: Reduce memory, not parameters for efficient on-device learning. In *Advances in Neural Information Processing Systems*, pages 11285–11297, 2020. 8

[12] Yuan Cao, Zhiying Fang, Yue Wu, Ding-Xuan Zhou, and Quanquan Gu. Towards understanding the spectral bias of deep learning. *arXiv preprint arXiv:1912.01198*, 2019. 4

[13] Daoyuan Chen, Liuyi Yao, Dawei Gao, Bolin Ding, and Yaliang Li. Efficient personalized federated learning via sparse model-adaptation. In *International Conference on Machine Learning*, pages 5234–5256. PMLR, 2023. 3

[14] Haokun Chen, Yao Zhang, Denis Krompass, Jindong Gu, and Volker Tresp. Feddat: An approach for foundation model finetuning in multi-modal heterogeneous federated learning. In *Proceedings of the AAAI Conference on Artificial Intelligence*, pages 11285–11293, 2024. 8

[15] Hong-You Chen and Wei-Lun Chao. On bridging generic and personalized federated learning for image classification. *arXiv preprint arXiv:2107.00778*, 2021. 8

[16] Jinyu Chen, Wenchao Xu, Song Guo, Junxiao Wang, Jie Zhang, and Haozhao Wang. Fedtune: A deep dive into efficient federated fine-tuning with pre-trained transformers. *arXiv preprint arXiv:2211.08025*, 2022. 2, 3

[17] Yiqiang Chen, Wang Lu, Xin Qin, Jindong Wang, and Xing Xie. Metafed: Federated learning among federations with cyclic knowledge distillation for personalized healthcare. *IEEE Transactions on Neural Networks and Learning Systems*, 2023. 8

[18] CA Coello Coello and Maximino Salazar Lechuga. Mopso: A proposal for multiple objective particle swarm optimization. In *Proceedings of the 2002 Congress on Evolutionary Computation. CEC'02 (Cat. No. 02TH8600)*, pages 1051–1056. IEEE, 2002. 7

[19] Liam Collins, Hamed Hassani, Aryan Mokhtari, and Sanjay Shakkottai. Exploiting shared representations for personalized federated learning. In *International conference on machine learning*, pages 2089–2099. PMLR, 2021. 8

[20] Kalyanmoy Deb, Amrit Pratap, Sameer Agarwal, and TAMT Meyarivan. A fast and elitist multiobjective genetic algorithm: Nsga-ii. *IEEE transactions on evolutionary computation*, 6(2):182–197, 2002. 7

[21] Marco Dorigo, Mauro Birattari, and Thomas Stutzle. Ant colony optimization. *IEEE computational intelligence magazine*, 1(4):28–39, 2006. 7

[22] Chen Dun, Cameron R Wolfe, Christopher M Jermaine, and Anastasios Kyrillidis. Resist: Layer-wise decomposition of resnets for distributed training. In *Uncertainty in Artificial Intelligence*, pages 610–620. PMLR, 2022. 3

[23] Alireza Fallah, Aryan Mokhtari, and Asuman Ozdaglar. Personalized federated learning with theoretical guarantees: A model-agnostic meta-learning approach. *Advances in neural information processing systems*, 33:3557–3568, 2020. 8

[24] Jonathan Frankle, David J. Schwab, and Ari S. Morcos. Training batchnorm and only batchnorm: On the expressive power of random features in cnns, 2021. 2

[25] Tao Guo, Song Guo, Junxiao Wang, Xueyang Tang, and Wenchao Xu. Promptfl: Let federated participants cooperatively learn prompts instead of models-federated learning in age of foundation model. *IEEE Transactions on Mobile Computing*, 2023. 8

[26] Song Han, Jeff Pool, John Tran, and William Dally. Learning both weights and connections for efficient neural network. *Advances in neural information processing systems*, 28, 2015. 8, 9, 10

[27] Haoyu He, Jianfei Cai, Jing Zhang, Dacheng Tao, and Bohan Zhuang. Sensitivity-aware visual parameter-efficient fine-tuning. In *Proceedings of the IEEE/CVF International Conference on Computer Vision*, pages 11825–11835, 2023. 8, 9, 10

[28] Agrin Hilmkil, Sebastian Callh, Matteo Barbieri, Leon René Sütfeld, Edvin Listo Zec, and Olof Mogren. Scaling federated learning for fine-tuning of large language models. In *International Conference on Applications of Natural Language to Information Systems*, pages 15–23. Springer, 2021. 3

[29] Neil Houlsby, Andrei Giurgiu, Stanislaw Jastrzebski, Bruna Morrone, Quentin De Laroussilhe, Andrea Gesmundo, Mona Attariyan, and Sylvain Gelly. Parameter-efficient transfer learning for nlp. In *International conference on machine learning*, pages 2790–2799. PMLR, 2019. 8

[30] Edward J Hu, yelong shen, Phillip Wallis, Zeyuan Allen-Zhu, Yuanzhi Li, Shean Wang, Lu Wang, and Weizhu Chen. LoRA: Low-rank adaptation of large language models. In *International Conference on Learning Representations*, 2022. 2, 8

[31] Arthur Jacot, Franck Gabriel, and Clément Hongler. Neural tangent kernel: Convergence and generalization in neural

networks. *Advances in neural information processing systems*, 31, 2018. 4

[32] Menglin Jia, Luming Tang, Bor-Chun Chen, Claire Cardie, Serge Belongie, Bharath Hariharan, and Ser-Nam Lim. Visual prompt tuning. In *Computer Vision – ECCV 2022: 17th European Conference, Tel Aviv, Israel, October 23–27, 2022, Proceedings, Part XXXIII*, page 709–727. Springer-Verlag, 2022. 2

[33] Gal Kaplun, Andrey Gurevich, Tal Swisa, Mazor David, Shai Shalev-Shwartz, and Eran Malach. Less is more: Selective layer finetuning with subtuning. *arXiv preprint arXiv:2302.06354*, 2023. 3

[34] Sai Praneeth Karimireddy, Satyen Kale, Mehryar Mohri, Sashank Reddi, Sebastian Stich, and Ananda Theertha Suresh. Scaffold: Stochastic controlled averaging for federated learning. In *International conference on machine learning*. PMLR, 2020. 1, 3, 5

[35] Wonjae Kim, Bokyung Son, and Ildoo Kim. Vilt: Vision-and-language transformer without convolution or region supervision. In *International conference on machine learning*, pages 5583–5594. PMLR, 2021. 1, 8

[36] Olga Kovaleva, Alexey Romanov, Anna Rogers, and Anna Rumshisky. Revealing the dark secrets of bert. *arXiv preprint arXiv:1908.08593*, 2019. 3

[37] Jason J Lau, Soumya Gayen, Asma Ben Abacha, and Dina Demner-Fushman. A dataset of clinically generated visual questions and answers about radiology images. *Scientific data*, 5(1):1–10, 2018. 8

[38] Cheolhyoung Lee, Kyunghyun Cho, and Wanmo Kang. Mixout: Effective regularization to finetune large-scale pretrained language models. In *International Conference on Learning Representations*. 3

[39] Jaejun Lee, Raphael Tang, and Jimmy Lin. What would elsa do? freezing layers during transformer fine-tuning. *arXiv preprint arXiv:1911.03090*, 2019. 3

[40] Namhoon Lee, Thalaiyasingam Ajanthan, and Philip HS Torr. Snip: Single-shot network pruning based on connection sensitivity. *arXiv preprint arXiv:1810.02340*, 2018. 2, 3, 8, 9, 10

[41] Sunwoo Lee, Tuo Zhang, and A Salman Avestimehr. Layerwise adaptive model aggregation for scalable federated learning. In *Proceedings of the AAAI Conference on Artificial Intelligence*, pages 8491–8499, 2023. 3

[42] Yoonho Lee, Annie S Chen, Fahim Tajwar, Ananya Kumar, Huaxiu Yao, Percy Liang, and Chelsea Finn. Surgical fine-tuning improves adaptation to distribution shifts. *arXiv preprint arXiv:2210.11466*, 2022. 2, 3, 8, 9, 10

[43] Brian Lester, Rami Al-Rfou, and Noah Constant. The power of scale for parameter-efficient prompt tuning. *arXiv preprint arXiv:2104.08691*. 2

[44] Bingbing Li, Zhenglun Kong, Tianyun Zhang, Ji Li, Zhengang Li, Hang Liu, and Caiwen Ding. Efficient transformer-based large scale language representations using hardware-friendly block structured pruning. *arXiv preprint arXiv:2009.08065*, 2020. 3

[45] Junnan Li, Ramprasaath Selvaraju, Akhilesh Gotmare, Shafiq Joty, Caiming Xiong, and Steven Chu Hong Hoi.

Align before fuse: Vision and language representation learning with momentum distillation. *Advances in neural information processing systems*, 34:9694–9705, 2021. 1, 8

[46] Junnan Li, Dongxu Li, Silvio Savarese, and Steven Hoi. Blip-2: Bootstrapping language-image pre-training with frozen image encoders and large language models. In *International conference on machine learning*, pages 19730–19742. PMLR, 2023. 1, 8

[47] Tian Li, Anit Kumar Sahu, Ameet Talwalkar, and Virginia Smith. Federated learning: Challenges, methods, and future directions. *IEEE signal processing magazine*, 37(3):50–60, 2020. 1, 3

[48] Xiang Lisa Li and Percy Liang. Prefix-tuning: Optimizing continuous prompts for generation. *arXiv preprint arXiv:2101.00190*, 2021. 2

[49] Dongze Lian, Daquan Zhou, Jiashi Feng, and Xinchao Wang. Scaling & shifting your features: A new baseline for efficient model tuning. *arXiv preprint arXiv:2210.08823*, 2022. 2

[50] Bo Liu, Li-Ming Zhan, Li Xu, Lin Ma, Yan Yang, and Xiao-Ming Wu. Slake: A semantically-labeled knowledge-enhanced dataset for medical visual question answering. In *2021 IEEE 18th International Symposium on Biomedical Imaging (ISBI)*, pages 1650–1654. IEEE, 2021. 8

[51] Haotian Liu, Chunyuan Li, Yuheng Li, and Yong Jae Lee. Improved baselines with visual instruction tuning. In *Proceedings of the IEEE/CVF Conference on Computer Vision and Pattern Recognition*, pages 26296–26306, 2024. 1, 8

[52] Renpu Liu, Cong Shen, and Jing Yang. Federated representation learning in the under-parameterized regime. *arXiv preprint arXiv:2406.04596*, 2024. 8

[53] Wang Lu, Jindong Wang, Yiqiang Chen, Xin Qin, Renjun Xu, Dimitrios Dimitriadis, and Tao Qin. Personalized federated learning with adaptive batchnorm for healthcare. *IEEE Transactions on Big Data*, 2022. 8

[54] Ekdeep Singh Lubana and Robert P Dick. A gradient flow framework for analyzing network pruning. In *International Conference on Learning Representations*. 2, 8, 9, 10

[55] Brendan McMahan, Eider Moore, Daniel Ramage, Seth Hampson, and Blaise Aguera y Arcas. Communication-efficient learning of deep networks from decentralized data. In *Artificial intelligence and statistics*. PMLR, 2017. 1, 2, 3

[56] John Nguyen, Kshitiz Malik, Maziar Sanjabi, and Michael Rabbat. Where to begin? exploring the impact of pre-training and initialization in federated learning. *arXiv preprint arXiv:2206.15387*, 4, 2022. 3

[57] Krishna Pillutla, Kshitiz Malik, Abdel-Rahman Mohamed, Mike Rabbat, Maziar Sanjabi, and Lin Xiao. Federated learning with partial model personalization. In *International Conference on Machine Learning*, pages 17716–17758. PMLR, 2022. 3

[58] John Rachwan, Daniel Zügner, Bertrand Charpentier, Simon Geisler, Morgane Ayle, and Stephan Günnemann. Winning the lottery ahead of time: Efficient early network pruning. In *International Conference on Machine Learning*, pages 18293–18309. PMLR, 2022. 3

[59] Nasim Rahaman, Aristide Baratin, Devansh Arpit, Felix Draxler, Min Lin, Fred Hamprecht, Yoshua Bengio, and

Aaron Courville. On the spectral bias of neural networks. In *International conference on machine learning*, pages 5301–5310. PMLR, 2019. 4

[60] Sylvestre-Alvise Rebuffi, Hakan Bilen, and Andrea Vedaldi. Efficient parametrization of multi-domain deep neural networks. In *Proceedings of the IEEE Conference on Computer Vision and Pattern Recognition*, 2018. 2

[61] Andreas Rücklé, Gregor Geigle, Max Glockner, Tilman Beck, Jonas Pfeiffer, Nils Reimers, and Iryna Gurevych. Adapterdrop: On the efficiency of adapters in transformers. *arXiv preprint arXiv:2010.11918*, 2020. 2, 8, 9, 10

[62] Pramit Saha, Divyanshu Mishra, Felix Wagner, Konstantinos Kamnitsas, and J. Alison Noble. Examining modality incongruity in multimodal federated learning for medical vision and language-based disease detection, 2024. 8

[63] Zhiqiang Shen, Zechun Liu, Jie Qin, Marios Savvides, and Kwang-Ting Cheng. Partial is better than all: Revisiting fine-tuning strategy for few-shot learning. In *Proceedings of the AAAI conference on artificial intelligence*, pages 9594–9602, 2021. 3

[64] Yubin Shi, Yixuan Chen, Mingzhi Dong, Xiaochen Yang, Dongsheng Li, Yujiang Wang, Robert Dick, Qin Lv, Yingying Zhao, Fan Yang, et al. Train faster, perform better: modular adaptive training in over-parameterized models. *Advances in Neural Information Processing Systems*, 36, 2024. 4

[65] Guangyu Sun, Matias Mendieta, Taojiannan Yang, and Chen Chen. Exploring parameter-efficient fine-tuning for improving communication efficiency in federated learning. 2022. 2

[66] Yi-Lin Sung, Varun Nair, and Colin A Raffel. Training neural networks with fixed sparse masks. *Advances in Neural Information Processing Systems*, 34:24193–24205, 2021. 2, 8, 9, 10

[67] Rishub Tamirisa, Chulin Xie, Wenxuan Bao, Andy Zhou, Ron Arel, and Aviv Shamsian. Fedselect: Personalized federated learning with customized selection of parameters for fine-tuning. In *Proceedings of the IEEE/CVF Conference on Computer Vision and Pattern Recognition*, pages 23985–23994, 2024. 8, 9, 10

[68] Yue Tan, Guodong Long, Lu Liu, Tianyi Zhou, Qinghua Lu, Jing Jiang, and Chengqi Zhang. Fedproto: Federated prototype learning across heterogeneous clients. In *Proceedings of the AAAI Conference on Artificial Intelligence*, pages 8432–8440, 2022. 8

[69] Hidenori Tanaka, Daniel Kunin, Daniel L Yamins, and Surya Ganguli. Pruning neural networks without any data by iteratively conserving synaptic flow. *Advances in neural information processing systems*, 33:6377–6389, 2020. 8, 9, 10

[70] Hugo Touvron, Matthieu Cord, Alaaeldin El-Nouby, Jakob Verbeek, and Hervé Jégou. Three things everyone should know about vision transformers. In *Computer Vision–ECCV 2022: 17th European Conference, Tel Aviv, Israel, October 23–27, 2022, Proceedings, Part XXIV*. Springer, 2022. 2

[71] Peter JM Van Laarhoven, Emile HL Aarts, Peter JM van Laarhoven, and Emile HL Aarts. *Simulated annealing*. Springer, 1987. 7

[72] Chaoqi Wang, Guodong Zhang, and Roger Grosse. Picking winning tickets before training by preserving gradient flow. *arXiv preprint arXiv:2002.07376*, 2020. 2, 3, 8, 9, 10

[73] Jianyu Wang, Qinghua Liu, Hao Liang, Gauri Joshi, and H Vincent Poor. Tackling the objective inconsistency problem in heterogeneous federated optimization. *Advances in neural information processing systems*, 33:7611–7623, 2020. 5

[74] Dingzhu Wen, Ki-Jun Jeon, and Kaibin Huang. Federated dropout—a simple approach for enabling federated learning on resource constrained devices. *IEEE wireless communications letters*, 11(5):923–927, 2022. 8, 9, 10

[75] Jian Xu, Xinyi Tong, and Shao-Lun Huang. Personalized federated learning with feature alignment and classifier collaboration. *arXiv preprint arXiv:2306.11867*, 2023. 8

[76] Runxin Xu, Fuli Luo, Zhiyuan Zhang, Chuanqi Tan, Baobao Chang, Songfang Huang, and Fei Huang. Raise a child in large language model: Towards effective and generalizable fine-tuning. *arXiv preprint arXiv:2109.05687*, 2021. 3

[77] Mingzhao Yang, Shangchao Su, Bin Li, and Xiangyang Xue. Exploring one-shot semi-supervised federated learning with pre-trained diffusion models. In *Proceedings of the AAAI Conference on Artificial Intelligence*, 2024. 2

[78] Xiyuan Yang, Wenke Huang, and Mang Ye. Fedas: Bridging inconsistency in personalized federated learning. In *Proceedings of the IEEE/CVF Conference on Computer Vision and Pattern Recognition*, pages 11986–11995, 2024. 8

[79] Sixing Yu, J Pablo Muñoz, and Ali Jannesari. Federated foundation models: Privacy-preserving and collaborative learning for large models. *arXiv preprint arXiv:2305.11414*, 2023. 2

[80] Elad Ben Zaken, Shauli Ravfogel, and Yoav Goldberg. Bitfit: Simple parameter-efficient fine-tuning for transformer-based masked language-models. *arXiv preprint arXiv:2106.10199*, 2021. 3

[81] Jianqing Zhang, Yang Hua, Hao Wang, Tao Song, Zhengui Xue, Ruhui Ma, and Haibing Guan. Fedala: Adaptive local aggregation for personalized federated learning. In *Proceedings of the AAAI Conference on Artificial Intelligence*, pages 11237–11244, 2023. 8

[82] Jianyi Zhang, Saeed Vahidian, Martin Kuo, Chunyuan Li, Ruiyi Zhang, Tong Yu, Guoyin Wang, and Yiran Chen. Towards building the federatedgpt: Federated instruction tuning. In *ICASSP 2024-2024 IEEE International Conference on Acoustics, Speech and Signal Processing (ICASSP)*. IEEE, 2024. 2

[83] Kaiyan Zhang, Ning Ding, Biqing Qi, Xuekai Zhu, Xinwei Long, and Bowen Zhou. Crash: Clustering, removing, and sharing enhance fine-tuning without full large language model. *arXiv preprint arXiv:2310.15477*, 2023. 3

[84] Lin Zhang, Li Shen, Liang Ding, Dacheng Tao, and Ling-Yu Duan. Fine-tuning global model via data-free knowledge distillation for non-iid federated learning. In *Proceedings of the IEEE/CVF conference on computer vision and pattern recognition*, pages 10174–10183, 2022. 3

[85] Michael Zhang, Karan Sapra, Sanja Fidler, Serena Yeung, and Jose M Alvarez. Personalized federated learn-

ing with first order model optimization. *arXiv preprint arXiv:2012.08565*, 2020. 8

[86] Pu Zhao, Fei Sun, Xuan Shen, Pinrui Yu, Zhenglun Kong, Yanzhi Wang, and Xue Lin. Pruning foundation models for high accuracy without retraining. *arXiv preprint arXiv:2410.15567*, 2024. 3

[87] Weiming Zhuang, Chen Chen, and Lingjuan Lyu. When foundation model meets federated learning: Motivations, challenges, and future directions. *arXiv preprint arXiv:2306.15546*, 2023. 2